Gain saturation and output power of distributed feedback lasers

1976 J. Phys. A: Math. Gen. 9 1309

(http://iopscience.iop.org/0305-4470/9/8/021)

J. Phys. A: Math. Gen., Vol. 9, No. 8, 1976. Printed in Great Britain.

Gain saturation and output power of distributed feedback lasers

Salvatore Solimeno and Giuseppe Mastrocinque

Instituto Electtrotecnico, Università di Napoli, Via Claudio 21, 80125 Napoli, Italia

Received 3 September 1974, in final form 1 March 1976

Abstract. A study is made of distributed feedback lasers operating above threshold. A set of non-linear differential equations governing the field distribution is obtained. Some properties of these equations are discussed analytically. Then the results of some numerical calculations are presented. As a result, it is shown that the field distribution inside the laser deviates notably from the linear case. Some explanations of what the analysis means in physical terms and how the different operating regimes are characterized are provided.

1. Introduction

Several papers have recently been published on the observation of laser action using a periodic structure as a mechanism for feedback. These devices exploit the fact that a periodic variation either in the complex dielectric constant or the thickness of the medium leads, when the Bragg condition is satisfied, to coupling of waves travelling in opposite directions. In conventional lasers the resonator is commonly formed by two end-mirrors terminating the laser medium. In distributed feedback (DFB) lasers the feedback mechanism is provided by Bragg scattering from a periodic spatial variation of the refractive index of the active medium, or of the gain itself. In addition, the grating-like nature of the device provides a filter mechanism which restricts the oscillations to a narrow spectral range.

Laser action in thin-film organic guides doped with rhodamine 6G dye has been observed by Bjorkholm and Shank (1972), Bjorkholm *et al* (1973) and Kogelnik *et al* (1973) and in multimode macroscopic liquid-dye guides by Zory (1972, 1973). More recently, Nakamura *et al* (1973, 1975a, 1975b) have reported stimulated emission in periodic structures etched into surfaces of GaAs crystals. Wang (1973) has observed laser oscillation in dye-impregnated polymer films with two-dimensional periodicities. Gas lasers using distributed feedback have also been proposed (Anderson and Shubert 1973).

Coupled-mode theory has been extensively used in analysing diffraction phenomena in optical waveguides perturbed by regular periodicities. Kogelnik and Shank (1971, 1972) have used this theory to discuss the feedback mechanism at work in DFB lasers. In so doing they have determined the frequency spectra of the DFB and the corresponding threshold gain for bulk media. Subsequently, Marcuse (1972) has examined the DFB laser oscillation in hollow dielectric waveguides. Kogelnik's results have been subsequently extended by Wang (1973, 1974) to two-layer waveguide structures.

In all these studies non-linear effects, such as gain saturation, have been neglected. The range of validity of these approximations is such that only the eigenvalue equation for the lasing frequencies and threshold gain characteristics can be derived. On the other hand, in this framework the intensity output cannot be related to the laser parameters such as gain, laser length, coupling coefficient (Kogelnik and Shank 1972) etc.

2. Preliminary considerations

Before examining analytically the behaviour of DFB lasers above threshold, a few remarks on the feedback mechanism at work in DFB and conventional lasers are premised.

When the feedback mechanism is achieved by imposing suitable boundary conditions at the laser cavity and the gain exceeds the threshold level, the laser field increases thus reducing the gain to the threshold value. During this process the field pattern does not change notably (in the first approximation). Conversely in a DFB device the field does not grow uniformly and its pattern changes in such a way as to provide a suitable energy exchange among the waves moving in opposite directions along the laser axis. As a result, in view of the field pattern relevance DFB devices are more difficult to examine above threshold than conventional ones.

When the electromagnetic field is confined by an optical resonator it can be described by a non-linear wave equation whose solution is a combination of modes depending on the cavity geometry only. On the contrary, the spatial configuration of the modes propagating in a DFB laser depends on the gain distribution in the active region. Therefore, it is useless trying to rely on a mode expansion technique for analysing the effects of gain saturation.

In conventional lasers the output characteristics are determined by describing the interaction of the laser field with the active medium in terms of radiation intensity, and, hence, the field phase distribution is neglected. The omission of phase relations is not rigorous because the phases of both direct and backward waves in the optical resonator are coupled. Nonetheless, Mikaeliane *et al* (1966) (see also Ratner 1972) have compared the results obtained using semiclassical equations and rate equations, thus showing that the difference between these two methods is insignificant from the practical point of view and does not appear in ordinary experiments.

Quite different is the situation for the DFB lasers. In this case the feedback is provided by a periodic change of the medium parameters on a scale comparable with the radiation wavelength. On the other hand, above threshold the gain profile is modulated by the coherent interference of the direct and backward waves. Since the period of this modulation is comparable with the former one, it is incorrect to neglect, *a priori*, this modulation by assuming uniform intensity on the wavelength scale.

Finally, as the field amplitude is non-uniform, the gain saturates non-uniformly along the active region. Therefore, no closed expression can be derived for the field configuration and we can only rely on numerical calculations.

The aim of this paper is to discuss some results relevant to DFB devices operating at the Bragg frequency exhibiting gain coupling. In the model used all geometrical factors have been neglected and the laser field has been assumed one-dimensional propagating back and forth along the z axis of the active region. The end reflectivity of the medium has been assumed equal to zero, as in the Shank–Kogelnik theory. However, this

limitation could easily be removed, thus allowing the investigation of the efficiency improvement due to non-vanishing mirror reflectivities, as shown in the linear case by Chinn (1973). The same applies to the gain coupling.

3. Above-threshold behaviour of DFB lasers

3.1. Generalities

The DFB laser is modelled as a guiding structure stretched along an axis, referred to in the following as the z axis, and extending from $z = -L/2$ to $z = L/2$. It may consist of a thin film sandwiched between a substrate and a top dielectric layer (eventually absent). Such a structure is able to confine the guided propagating mode (see figure 1) prevalently in the active region, thus allowing the amplification process to make up for the losses by leakage through the substrate and top layer.

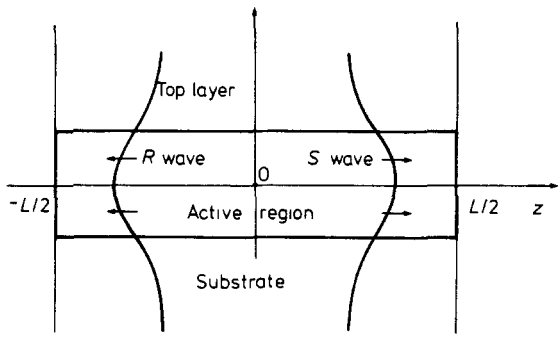

Figure 1. Schematic diagram of the DFB laser.

Slightly different geometries may also be considered relevant to the present analysis. In the recent proposals by Akhmanov and Lyakhov (1974) and Fisher (1974) to use DFB structures for generation in the ultraviolet and x-ray region, the active material is a gas or a crystal bounded in suitable ways. As regards gain saturation effects, these lasers exhibit strong similarities with the above mentioned thin-film DFB lasers.

Feedback mechanism forcing guided waves to travel back and forth may be provided by surface periodicity, waveguide index periodicity or gain periodicity. In particular we shall consider gain periodicity only. This may be accomplished by using two coherent pump beams which interfere in the active region (see for example Zlenko *et al* 1974). However, the interested reader will easily find out how to extend the present analysis to different types of modulation.

We represent the laser field as a superposition of TE and TM modes. The monochromatic ($e^{-i\omega t}$) field $\boldsymbol{E}$ is described by a complex amplitude $V(z)$ and a mode profile $\mathscr{E}(x, y)$ (normalized to carry one unit of power):

$$\boldsymbol{E}(x, y, z) = V(z)\mathscr{E}(x, y). \tag{1}$$

$\mathscr{E}$ depends on the transverse geometry of the guiding structure, whereas $V(z)$ satisfies the one-dimensional wave equation (see e.g. Felsen and Marcuvitz 1973):

$$\frac{d^2V}{dz^2} + i\omega\mu_0\sigma V + \frac{\omega^2 V}{v_f^2} = -\omega^2\mu_0 P. \tag{2}$$

The conductivity σ is an *ad hoc* factor accounting for the energy leakage through the boundaries (Tien 1971), while P stands for the complex amplitude of the polarization vector

$$\boldsymbol{P}(x, y, z) = P(z)\mathscr{E}(x, y).$$

On the other hand, P is related to V through (see for example Yariv 1975)

$$P = -\frac{\mathrm{i}AV}{\omega^2\mu_0}\left(1-\delta\frac{|V|^2}{\mathscr{I}_s}\mathscr{E}^2\right) \tag{3}$$

where A is proportional to the small-signal gain, and δ is a factor depending on the type of laser transition broadening. In passing, we note that equation (3) is valid for laser signals small with respect to the saturation intensity $\mathscr{I}_s$.

According to (3), the relation between P and V depends on (x, y) coordinates as well. However, if we assume that $\mathscr{E}$ does not change noticeably across the active region, the (x, y) dependence of the above constitutive relation can be neglected. That is the case in which the laser field extends in the substrate, namely the lowest-order mode is propagating. In any case, our simplifying assumption is in line with accepted laser theories (see Sargent *et al* 1974, chap. 8).

Substitution of (3) in (2) yields

$$\frac{\mathrm{d}^2u}{\mathrm{d}z^2}+k^2u = \mathrm{i}[A(1-|u|^2)-\omega\mu_0\sigma]u \tag{4}$$

where $k = \omega/v_f$ and $u = V\mathscr{E}(\delta/\mathscr{I}_s)^{1/2} < 1$.

Now, if A depends on z as

$$A(z) = A_0(1+2\kappa\cos 2\beta_0 z)$$

with $\kappa \ll 1$, equation (4) reads

$$\frac{\mathrm{d}^2u}{\mathrm{d}z^2}+(k^2+\mathrm{i}\omega\mu_0\sigma)u-\mathrm{i}A_0(1+2\kappa\cos 2\beta_0 z)(1-|u|^2)u = 0. \tag{5}$$

3.2. Laser oscillation description in terms of coupled modes

If we neglect the non-linear term of equation (5), u may be represented as a summation over the set of all the discrete modes, whose propagation constants are solutions of an infinite-dimensional determinantal equation (see Elachi 1971 and Elachi and Yeh 1973, Elachi *et al* 1974). For $k \simeq \beta_0$ (Bragg resonance) the field can be described by using two modes of slowly varying amplitudes. As an extension of this coupled-mode approach, we write the electric field as the sum

$$u(z) = R(z)\,\mathrm{e}^{-\mathrm{i}\beta_0 z} + S(z)\,\mathrm{e}^{\mathrm{i}\beta_0 z} \tag{6a}$$

where

$$\beta_0^2 R \gg \mathrm{d}^2R/\mathrm{d}z^2, \qquad \beta_0^2 S \gg \mathrm{d}^2S/\mathrm{d}z^2 \tag{6b}$$

and

$$S(-L/2) = R(L/2) = 0. \tag{6c}$$

The S wave represents a field travelling in the positive direction of the z axis. The opposite holds for R.

Inserting (6) into (5) and capitalizing on (6*b*), we find

$$\begin{aligned}
&e^{-i\beta_0 z}\{R[k^2-\beta_0^2+i\omega\mu_0\sigma-iA_0(1-|R|^2-2|S|^2)]\\
&\quad -i\kappa A_0[S(1-|R|^2-|S|^2)-R(RS^*+R^*S)]-2i\beta_0 dR/dz\}\\
&\quad +e^{i\beta_0 z}\{S[k^2-\beta_0^2+i\omega\mu_0\sigma-iA_0(1-2)|R|^2-|S|^2)]\\
&\quad -i\kappa A_0[R(1-|R|^2-|S|^2)-S(RS^*+R^*S)]+2i\beta_0 dS/dz\}=0, \qquad (7)
\end{aligned}$$

having neglected the terms containing the phase factors $e^{\pm 3i\beta_0 z}$ and $e^{\pm 5i\beta_0 z}$, as $\kappa \ll 1$.

Now, by defining

$$\zeta \equiv \frac{zA_0}{2\beta_0} \qquad (8a)$$

$$a_1 \equiv 1-\frac{\omega\mu_0\sigma}{A_0}, \qquad a_2 \equiv \frac{k^2-\beta_0^2}{A_0}, \qquad a \equiv a_1+ia_2 \qquad (8b)$$

$$I \equiv |R|^2+|S|^2, \qquad D \equiv |S|^2-|R|^2, \qquad T \equiv |RS| \qquad (8c)$$

$$R \equiv |R|e^{i\phi}, \qquad S \equiv |S|e^{i\psi}, \qquad \alpha^- \equiv \psi-\phi, \qquad \alpha^+ \equiv \psi+\phi \qquad (8d)$$

and starting from (7), we find (see appendix)

$$dI/d\zeta = 2(a_1-I-2\kappa T\cos\alpha^-)D \qquad (9a)$$

$$dD/d\zeta = 2(a_1-I)I+4T[\kappa\cos\alpha^-(1-2I)-T] \qquad (9b)$$

$$dT/d\zeta = -D[\kappa(1-I)\cos\alpha^- - T] \qquad (9c)$$

$$d\alpha^-/d\zeta = 2a_2+\kappa\sin\alpha^- DT^{-1}(1-I) \qquad (9d)$$

$$d\alpha^+/d\zeta = \kappa\sin\alpha^- IT^{-1}(1-I) \qquad (9e)$$

with boundary conditions

$$I(-L/2) = I(L/2) = I_{out} \qquad (9f)$$

$$D(-L/2) = -D(L/2) = -I_{out} \qquad (9g)$$

$$T(-L/2) = T(L/2) = 0 \qquad (9h)$$

$$\alpha^-(-L/2) = 0. \qquad (9i)$$

The symmetry of the device limits the search for solutions of (9) to the symmetric ($u(-z)=u(z)$) and antisymmetric ($u(z)=-u(z)$) field configurations. Accordingly, it is easy to verify that this is tantamount to imposing

$$\alpha^+(z) = \alpha^+(-z), \qquad \alpha^-(z) = \alpha^-(z) \qquad (9j)$$

$$I(z) = I(-z), \qquad D(z) = -D(-z), \qquad T(z) = T(-z). \qquad (9k)$$

For $k=\beta_0$ and ω equal to the laser transition frequency, A_0 is real, $a_2=0$ and (9*d*) simplifies as

$$d\alpha^-/d\zeta = \kappa\sin\alpha^- DT^{-1}(1-I). \qquad (10)$$

If $\alpha^- \neq 0$, (10) can be divided by (9*e*) yielding

$$\frac{d\alpha^-/d\zeta}{d\alpha^+/d\zeta} = \frac{D}{I}. \qquad (11)$$

Since the left-hand side is an even function of ζ (cf equation (9*j*)) while the right-hand side is an odd one (cf equation (9*k*)), α^- must be constant and equal to $n\pi$ (cf equation (10)). This holds true for each interval in which T does not vanish. If we allow T to become negative as well, we can put $\alpha^- = 0$ everywhere and equation (9) read

$$dI/d\zeta = 2(a_1 - I - 2\kappa T)D \tag{12a}$$

$$dD/d\zeta = 2(a_1 - I)I + 4T[\kappa(1-2I) - T] \tag{12b}$$

$$dT/d\zeta = -D[\kappa(1-I) - T]. \tag{12c}$$

4. Solution of the differential system for the coupled modes

4.1. Reduction of the differential system to canonical form

As a preliminary step we replace equation (12*b*) with

$$I^2 = 4T^2 + D^2. \tag{13}$$

Now, if we introduce a new variable t such that $dt = D d\zeta$, (12*a*) and (12*c*) become a plane autonomous system with a saddle point (see Birkhoff and Rota 1969) in

$$I_S = \frac{a_1 - 2\kappa^2}{1 - 2\kappa^2} \tag{14a}$$

$$T_S = \kappa \frac{1 - a_1}{1 - 2\kappa^2}. \tag{14b}$$

By reducing (12*a*) and (12*c*) to canonical form with the transformation

$$I = \tfrac{4}{3}\kappa x_1 + x_2 + I_S \tag{15a}$$

$$T = x_1 - \tfrac{1}{3}\kappa x_2 + T_S \tag{15b}$$

we obtain (as $\kappa \ll 1$)

$$dx_1/d\zeta = Dx_1 \tag{16a}$$

$$dx_2/d\zeta = -2Dx_2 \tag{16b}$$

$$D^2 = I^2 - 4T^2. \tag{16c}$$

The integral curves

$$x_1^2(\zeta)x_2(\zeta) = \text{constant} \tag{17}$$

of equations (16*a*) and (16*b*) look like a family of similar hyperbolas as shown in figures 2(*a*) and 2(*b*).

Because of equation (9*k*), $D(\zeta)$ can vanish $2n+1$ times in the interval $(-L/2, L/2)$. If we refer for simplicity to the fundamental mode of oscillation (i.e. $n = 0$), D will be positive for $\zeta > 0$. Accordingly, integrating (16*a*) from 0 to $L/2$ yields

$$\int_{x_1(0)}^{x_1(LA_0/4\beta_0)} \frac{dx_1}{D(x_1)x_1} = \frac{LA_0}{4\beta_0} \tag{18}$$

where $D(x_1)$ is obtained from (16*c*) expressing I and T as functions of x_1 and $x_2 = x_1^{-2} \times$ constant. The integrand of (18) demands some attention since D vanishes for

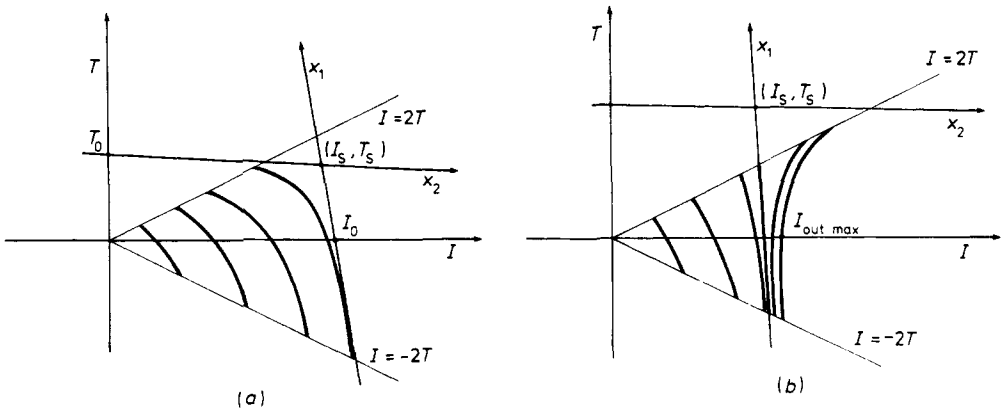

Figure 2. (*a*) Graph of the integral curves of the differential system (16). The coordinate system (x_1, x_2) centred at (I_S, T_S) (cf equation (14)) is also shown. The axes x_1 and x_2 intersect the I and T axes at the points I_0 and T_0 respectively (cf equations (19)). D and z vanish at the crossing points of the integral curves with the straight lines $I = \mp 2T$, whereas the points of the I axis correspond to $z = \mp L/2$. (*b*) Graph of the integral curves of the differential system (16) for $2T_S > I_S$. Since the integral curves must intersect the lines $I = \mp 2T$, in order to represent a physical situation, only those on the left of the curve tangent to $I = 2T$ are shown.

$x_1 = x_1(0)$. A simple analysis will show that $D(x_1) = O[(x_1 - x_1(0))^{1/2}]$; consequently, this singularity can be easily removed. Anyway, some care must be taken when (18) is integrated numerically.

For the sake of clarity, we note that according to our definitions (cf equation (5)) the quantity $a_1 A_0/2\beta_0 = \alpha$ is the average small-signal gain of the medium, while $A_0\kappa/\beta_0 = \alpha_1$ is the amplitude of the oscillating gain component. Accordingly, the right-hand side of (18) can be rewritten as $\alpha L/2a_1$.

Because of the saddle-point singularity, the differential system (16) admits three distinct classes of solutions according to whether $x_2 < 0$, $x_2 = 0$, $x_2 > 0$. In view of this, capitalizing on (14) and (15) and taking into account that $x_1 < 0$, we find

$$I - \tfrac{4}{3}\kappa T \lesseqgtr I_S - \tfrac{4}{3}\kappa T_S \equiv I_0 \tag{19a}$$

$$\tfrac{1}{3}\kappa I + T < \tfrac{1}{3}\kappa I_S + T_S \equiv T_0. \tag{19b}$$

In particular, by specializing (19) to I_{out} and $I(0)$, we obtain some upper and lower bounds for these quantities (see table 1).

Table 1. Upper and lower bounds for various quantities.

$\gamma = a_1/2\kappa$	x_1	I_{out}	$I(0)$	$I_{out\ max}$
>1	<0	$<I_0$	$<(1-\frac{2}{3}\kappa)^{-1} I_0$	$=I_0$
<1	<0	$<I_0$	$<(1-\frac{2}{3}\kappa)^{-1} I_0$	$=I_0$
<1	$=0$	$=I_0$	$=(1-\frac{2}{3}\kappa)^{-1} I_0$	$=I_0$
<1	>0	$>I_0$	$>(1-\frac{2}{3}\kappa)^{-1} I_0$	$>I_0$

4.2. Analysis of some particular cases

In this subsection we illustrate some analytic solution of the system (12) and discuss some features of the I_{out} dependence on a_1, κ and L.

As a preliminary case we assume $a_1 \ll 1$, which is tantamount to imposing the gain very close to the loss factor. Under this hypothesis and the additional condition $a_1 > 2\kappa^2$, we find that $I_S \simeq a_1$, $T_S \simeq \kappa$ and

$$T(\zeta) = \kappa\left[1 - \left(\frac{a_1 - I_{out}}{a_1 - I(\zeta)}\right)^{1/2}\right]. \tag{20}$$

Then, by substitution of x_1 with I in the integral (18) we obtain

$$\int_{I(0)}^{I_{out}} \frac{2\kappa \, dI}{(a_1 - I)(I^2 - 4\kappa^2\{1 - [(a_1 - I_{out})/(a_1 - I)]^{1/2}\}^2)^{1/2}} = \frac{\alpha_1 L}{2} \tag{21}$$

where $I(0)$ is related to I_{out} through (20). This equation displays an important property, that is, $\alpha_1 L/2$ ('coupling strength' in Kogelnik and Shank 1972) depends on $a_1/2\kappa \equiv \gamma$ and I_{out}/a_1 only.

As far as $\gamma > 1$, I_{out}/a_1 cannot exceed $I_0/a_1 \approx 1$ (cf table 1), whereas for $\gamma < 1$, I_{out} is bounded above by

$$I_{out} < I_{out\,max} \equiv a_1\left(1 + \frac{4}{27}\frac{1}{\gamma}(1-\gamma)^3\right) \tag{22a}$$

and the corresponding value of $I_{max}(0)$ is given by

$$I_{max}(0) = a_1\left(\frac{1}{3\gamma} + \frac{2}{3}\right). \tag{22b}$$

The interested reader is referred to Rigrod (1963) for the discussion of a similar situation occurring in conventional lasers.

Another particular solution is obtained by assuming $x_2 = 0$. In this case we have (cf figure 2(*b*))

$$I - I_S = \tfrac{4}{3}\kappa(T - T_S) \tag{23}$$

and the integral (18) can be evaluated analytically:

$$\frac{a_1}{2T_S(1-g^2)^{1/2}}\left[\frac{\pi}{2} + \tan^{-1}\left(\frac{g}{(1-g^2)^{1/2}}\right)\right] = \frac{\alpha L}{2} \tag{24}$$

where $g \equiv I_S/2T_S$. In particular, when $I_S \approx a_1$ and $T_S \approx \kappa$, g coincides with γ.

A situation of particular interest is that for which $\kappa = 0$. In this case, the laser operates without any external modulation of the gain. The spatial holes burned by the sinusoidally varying laser field (see Sargent *et al* 1974, p 105) induce a coupling between the counter-running fields. A similar phenomenon, such as the generation of sidebands by two strong input signals in dilute laser amplifying media, has been investigated by Close (1967). For $\kappa = 0$, in view of equations (14) and (15), equation (17) reads

$$T^2(I - a_1) = \text{constant}.$$

Consequently, equations (12) admit a solution only if T does not vanish at the laser boundaries. In fact, if $T(\pm L/2) = 0$, constant $= 0$. This, in turn, implies $T = 0$ or $I = a_1$ in the active region. In the former case one of the waves R and S would vanish. In the

latter case, since $x_2 = 0$, equation (24) yields $\alpha L/2 = \infty$. Accordingly, the laser can operate only if the end reflectivity is different from zero.

Finally, as $I_{out} \to 0$, equation (18) simplifies to

$$\int_{\kappa/(a_1+\kappa)}^{1} \frac{dx}{[x^2-\kappa^2(x-1)^2/a_1^2]^{1/2}} = \alpha L \tag{25}$$

with $x = I/I_{out}$, thus giving (see Gradshteyn and Ryzhik 1965)

$$\frac{2\gamma}{(4\gamma^2-1)^{1/2}} \sinh^{-1}[(4\gamma^2-1)^{1/2}] = \alpha L \tag{26}$$

in agreement with equation (18) of Kogelnik and Shank (1972).

5. Discussion of some numerical results

We have made some numerical integrations of the non-linear system (12) by assuming $a_1 \ll 1$ and $a_1 = 1$.

In particular, we have calculated the integral (18) for $a_1 \ll 1$ by assuming different values of $\gamma(=\alpha/\alpha_1)$ and the relative values of I_{out} are plotted as functions of αL in figure 3. We note that for $\gamma < 1$, I_{out}/a_1 increases rapidly in relation to αL; this is in contrast to what happens for $\gamma > 1$. Accordingly, for assigned a_1, it seems preferable to increase κ (modulation depth) as much as possible, in order to augment the laser output. In so doing, it is possible to extract a beam having an intensity of the order of $I_{out\,max}$ (cf equation (22)), without exceeding appreciably the threshold length. In addition, it is worth quoting Kogelnik and Shank (1972) where it is noted that a high value of γ leads to considerable mode discrimination in favour of the mode oscillating at the Bragg resonance. In view of both these circumstances a high γ is recommended for a gain-coupled DFB laser.

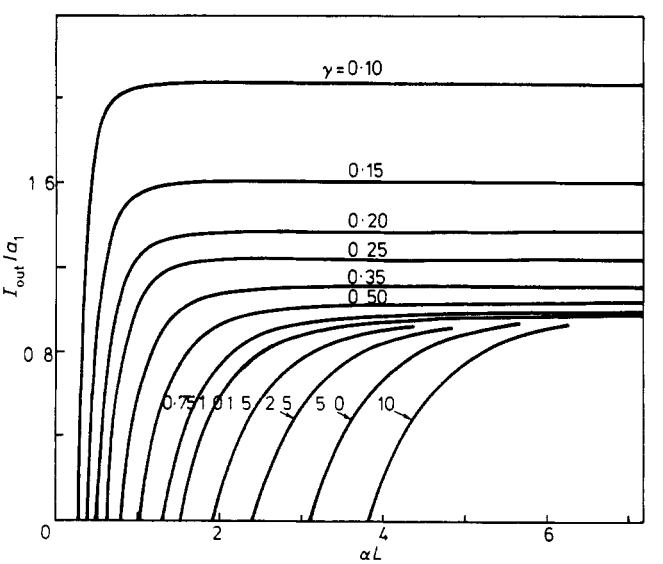

Figure 3. Graph of the normalized intensity output I_{out}/a_1 against the gain αL for $a_1 \ll 1$ and different values of $\gamma = \alpha/\alpha_1$.

Our former conclusions are based on the hypothesis of small a_1. To get a better insight, we have solved the differential system for $a_1 = 1$ obtaining the graph of figure 4. In keeping with the coupled-mode approximation, which implies $\kappa \ll 1$, only values of γ ranging from 3·125 upwards have been considered. On the other hand, the curves of figure 4 extend from $I_{out} = 0$ to 1. Since equation (5) is valid for small values of I, these diagrams are consistent with our model only near the abscissa axis. Also in this case we note a rapid increase of I_{out} for a slight change of the gain αL, thus confirming the previous conclusions in the absence of losses.

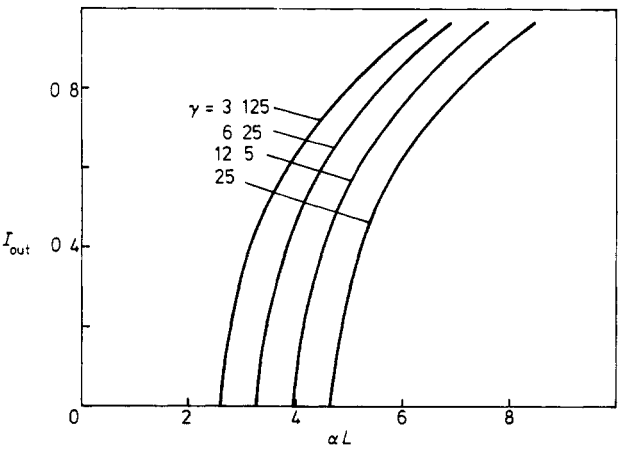

Figure 4. Graph of the normalized intensity output I_{out} against the gain αL for $a_1 = 1$ and different values of γ.

In figure 5 we have presented the data of figure 3 in a different way by plotting αL as a function of the coupling strength $\alpha_1 L$ for different values of I_{out}/a_1. For $I_{out} = 0$, the relative graph (cf equation (26)) coincides with the threshold diagram of Kogelnik and Shank (1972). The curve for $x_2 = 0$ ($I_{out} \approx a_1$) has been obtained by capitalizing on equation (24), whereas the other two have been obtained from figure 3. We observe that all the curves converge to the point π on the $\alpha_1 L$ axis. For a gain αL of the order of

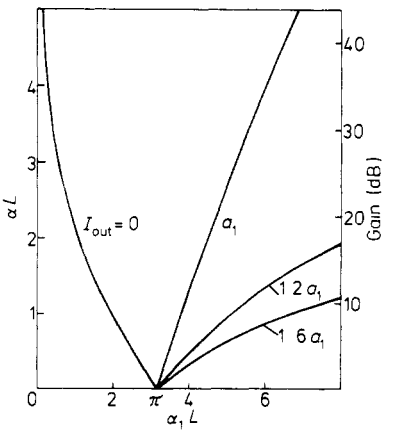

Figure 5. Graph of αL against $\alpha_1 L$ for different values of I_{out} and $a_1 \ll 1$.

10 dB, we have to increase the coupling strength up to 35 dB in order to achieve an intensity output equal to a_1. Alternatively, with a gain of about 4 dB and a coupling strength of 35 dB, an intensity of $1{\cdot}6\ a_1$ is obtained.

Figure 6 refers to the case $a_1 = 1$. We observe a marked difference from the former. In fact, the curves for constant I_{out} diverge as the coupling strength increases. In addition, for assigned gain the coupling strength is a rapidly increasing function of I_{out}.

In figure 7 the intensity distribution along the laser axis for a gain equal to 3 has been plotted for different γ.

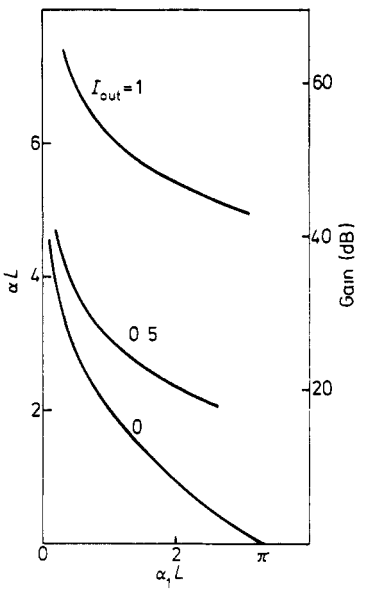

Figure 6. Graph of αL against $\alpha_1 L$ for $a_1 = 1$ and different values of I_{out}.

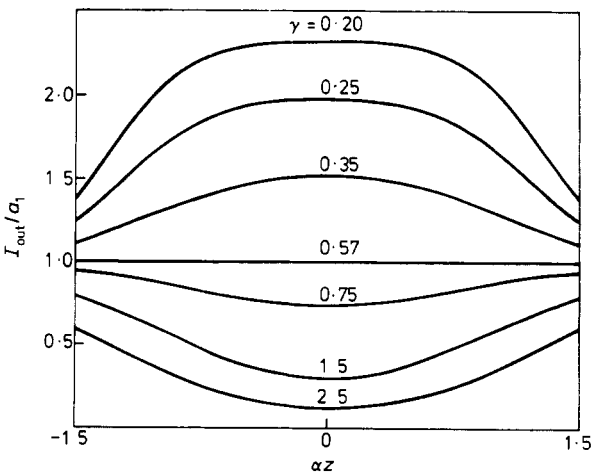

Figure 7. Graph of the intensity distribution I along the laser axis for $\alpha L = 3$ and different values of γ.

6. Conclusions

A non-linear analysis of a gain-coupled DFB laser has been presented. Some analytical results have been discussed, which provide some information about the output intensity as a function of the laser length, gain and modulation depth. In addition, graphs of some numerical calculations have been reported and looked at.

To simplify the analysis two different operating regimes have been looked at. In the first case, characterized by a loss/gain ratio of the order of unity, it has been shown that the laser output and the field configuration inside the active region only depend on the gain factor αL and the coupling strength $\alpha_1 L$. In particular, some parametric considerations have been presented, showing that for assigned a_1, a small γ leads to a high output I_{out} for a gain slightly greater than its threshold value. Alternatively, for given length L, a small γ leads to a poor output coupling, that is the output intensity is much smaller than the average intensity inside the laser.

The primary conclusions that can be drawn from this analysis are that a small value of γ leads to a high output intensity in addition to a strong mode discrimination.

Acknowledgments

Particular thanks are due to Professor A Yariv for helpful comments. One of us (GM) would like to thank Professor L Henry for the warm hospitality offered at his Laboratory and the Italian National Council of Research for financial assistance. This work was partially sponsored by the Italian National Council of Research.

Appendix

Equation (7) splits in two equations:

$$dR/d\zeta = R[-a+|R|^2+2|S|^2]-\kappa[S(1-|R|^2-|S|^2)-R(RS^*+R^*S)], \tag{A.1}$$

$$-dS/d\zeta = S[-a+|S|^2+2|R|^2]-\kappa[R(1-|S|^2-|R|^2)-S(R^*S+RS^*)], \tag{A.2}$$

having made use of equations (8). Multiplying (A.1) by R^* and retaining the real part yields

$$d|R|^2/d\zeta = (I-D)(-a_1+\tfrac{3}{2}I+\tfrac{1}{2}D)-2\kappa T\cos\alpha^-(1-2I+D). \tag{A.3}$$

Analogously for $|S|^2$:

$$-d|S|^2/d\zeta = (I+D)(-a_1+\tfrac{3}{2}I-\tfrac{1}{2}D)-2\kappa T\cos\alpha^-(1-2I-D). \tag{A.4}$$

Adding and subtracting (A.3) and (A.4) we obtain (9*a*) and (9*b*). Premultiplying (A.1) by S^* and (A.2) by R^*, adding the two resulting equations and splitting it in real and imaginary parts, we get equations (9*c*) and (9*d*). Premultiplying (A.1) by S and (A.2) by R and proceeding in the same way we obtain equation (9*e*).

References

Akhmanov S A and Lyakhov G A 1974 *JEPT Lett.* **19** 251–3

Anderson D B and Shubert R 1973 *Rockwell International Company, Int. Tech. Rep.* No. C72-650.101501

Birkhoff G and Rota G C 1969 *Ordinary Differential Equations* (Waltham, Ma: Blaisdell)
Bjorkholm J E and Shank C V 1972 *IEEE J. Quant. Electron.* **8** 833–8
Bjorkholm J E, Sosnowski T P and Shank C V 1973 *Appl. Phys. Lett.* **22** 132–4
Chinn S R 1973 *IEEE J. Quant. Electron.* **9** 574–9
Close D H 1967 *Phys. Rev.* **153** 360–71
Elachi C 1971 *PhD Thesis* California Institute of Technology
Elachi C and Yeh C 1973 *J. Appl. Phys.* **44** 3146–52
Elachi C, Evans G and Yeh C 1974 *Jet Propulsion Laboratory Internal Report*
Felsen L and Marcuvitz N 1973 *Radiation and Scattering of Waves* (Englewood Cliffs, NJ: Prentice-Hall)
Fisher R A 1974 *Appl. Phys. Lett.* **24** 598–9
Gradshteyn I S and Ryzhik I M 1965 *Table of Integrals, Series and Products* (New York: Academic)
Kogelnik H and Shank C V 1971 *Appl. Phys. Lett.* **18** 152–4
——— 1972 *J. Appl. Phys.* **43** 2327–35
Kogelnik H, Shank C V and Bjorkholm J E 1973 *Appl. Phys. Lett.* **22** 135–7
Marcuse D 1972 *IEEE J. Quant. Electron.* **8** 661–9
Mikaeliane A L, Ter-Mikaeliane M L, Turkov J G and Djatchenko V V 1966 *IEEE J. Quant. Electron.* **2** 363–5
Nakamura M, Aiki K, Umeda J, Katzir A, Yariv A and Yen H W 1975a *IEEE J. Quant. Electron.* **11** 436–41
———1975b *Appl. Phys. Lett.* **27** 403–5
Nakamura M, Yariv A, Yen H W, Somekh S and Garwin H L 1973 *Appl. Phys. Lett.* **22** 515–6
Ratner A M 1972 *Spectral, Spatial and Temporal Properties of Lasers* (New York: Plenum) pp 67–70
Rigrod W W 1963 *J. Appl. Phys.* **34** 2602–9
Sargent M, Scully M O and Lamb W E 1974 *Laser Physics* (Reading, Mass.: Addison Wesley)
Tien P K 1971 *Appl. Opt.* **10** 2395–9
Wang S 1973 *J. Appl. Phys.* **44** 767–80
——— 1974 *IEEE J. Quant. Electron.* **10** 413–27
Yariv A 1975 *Quantum Electronics* 2nd edn (New York: Wiley)
Zlenko A A, Prokhorov A M and Sychngov V A 1974 *Sov. J. Quant. Electron.* **3** 493–5
Zory P 1972 *Integrated Optics Conf. Dig. Tech. Pap.* (Washington: Optical Society of America)
——— 1973 *Appl. Phys. Lett.* **22** 125–8